

MRE Determination of the Lamé Constants by Simultaneous Visualization of P- and S-waves

B. Zhang¹, J. Zhuo¹, G. M. Beache¹

¹Cardiovascular Imaging and Physiology Center, Diagnostic Radiology Department, University of Maryland Medical Center, Baltimore, MD, United States

Synopsis

Magnetic resonance elastography (MRE) estimation of shear modulus (s-wave) of biomaterials has been documented. We now report the simultaneous detection of the longitudinal (p-) and shear waves, which is necessary to completely specify the material properties of a solid. A periodic vibration was applied axially along a cylindrical phantom (6% gelatin; 50 Hz), resulting in a p-wave traveling along the axial direction, and an ortho-normal s-wave. P- and s-wave vibrations were encoded using axial motion-sensitization. Wave speeds and thus the 2 independent Lamé constants were estimated. Measured Poisson ratio was 0.38 ± 0.09 vs. 0.5, assumed for incompressible solids.

Introduction

Evaluation of material properties of solids is important both for industrial applications and in biomedicine. Determination of the two independent Lamé constants (λ , μ) is necessary and sufficient for the complete specification of elastic, isotropic solids. Non-invasive magnetic resonance elastography (MRE) has been used to estimate the shear modulus [1], a Lamé constant. An algebraic inversion method [2], as well as finite element-based inversion scheme [3], have been used to indirectly obtain estimates of the 2nd Lamé constant. In the present study we implemented a method to directly measure the 2 Lamé constants, and derive an estimate for the Poisson ratio.

Material and Methods

Theory For isotropic, elastic materials, the Navier equilibrium equation, in terms of displacement, yields: $\mu \nabla \times (\nabla \times u) + (\lambda + \mu) \nabla (\nabla \cdot u) = \rho \partial^2 u / \partial t^2$, where; λ , μ are the Lamé constants, u is the displacement, t is the time, ρ is the density of the material, and we neglect gravity. This equation can be thought of as separable into a dilatational term, $(\lambda + \mu) \nabla (\nabla \cdot u)$, and a rotational term, $\mu \nabla \times (\nabla \times u)$. Further, using the Helmholtz decomposition, the displacement u can be expressed as a sum of two components: $u = \nabla p + \nabla \times s$, where p is a compressional scalar potential, and s is an equivoluminal vector potential. By substituting the expression for u into the Navier equation, we obtain two independent wave equations: $\nabla^2 p = [\rho / (\lambda + 2\mu)] \cdot \partial^2 p / \partial t^2$ and $\nabla^2 s = (\rho / \mu) \cdot \partial^2 s / \partial t^2$. Thus the general solution simplifies into ortho-normal p- and s-waves.

From the form of the wave equations, the wave speeds are given by: $c_s = \sqrt{\mu / \rho}$ and $c_l = \sqrt{(\lambda + 2\mu) / \rho}$, where c_s and c_l are the transverse- and longitudinal- wave speeds, respectively. From continuum mechanics, given any 2 independent material constants for elastic isotropic materials, the other material constants (Poisson ratio, ν , and Young modulus, Y) can be derived. Thus the material constants can be expressed as: $\mu = \rho c_s^2$, $\lambda = \rho c_l^2 - 2\rho c_s^2$, $\nu = 1 - 1 / (2 - 2(c_s / c_l)^2)$, and $Y = 4\rho c_s^2 - \rho c_l^2 / (c_l^2 - c_s^2)$.

Phantom To derive a phantom approximating biomaterials we used 6% gelatin (Type A; EC No. 232-554-6; Porcine skin, 300; Bloom Sigma Chemical Co.). Shape was cylindrical. We applied a 50 Hz, periodic, axial vibration to the phantom, using an electro-mechanical actuator, to generate the material particle vibrations (Figure 1).

Imaging MRE acquisitions were done at 1.5T, (40 mT/m peak gradients) (Eclipse; Philips Medical System, Cleveland, Ohio), using a modified spin-echo sequence, with bipolar motion encoding gradients [4], oriented along the applied vibration. Parameters included; TR/TE 400/50 ms, slice thickness 5 mm, FOV 16cm, and acquisition matrix 128x256 (interpolated in the phase direction, to yield a 256x256 matrix, or 0.625x0.625 mm² pixel resolution). 2-D phase maps were generated, in an image plane encompassing the motion-sensitive direction.

Results

Motion encoded data yielded 2-D phase maps (Figure 2). Line profiles of the intensity were obtained from the phase maps, to directly estimate wavelengths. Note that "noise" (extending beyond the phantom) has been filtered. Wavelength is defined as the crest to crest- or, alternatively, trough to trough- distance. We thus obtained a half-wavelength; 76 ± 12 pixels (47.5 ± 7.5 mm) for the longitudinal wave, and a full-wavelength; 66 ± 8 pixels (41 ± 5 mm) for the shear wave (Figure 2b, 2c). From the known frequency of vibration, and assuming a density of 1000 Kg/m³, which is good to 2%, for our applications, we obtain longitudinal and transverse wave speeds of 4.75 ± 0.75 m/s, and 2.06 ± 0.25 m/s, respectively. Material constants (λ , μ , Y , ν) are summarized in Table 1. Standard errors are reported, and were derived using error propagation analysis. Literature values from a recent report of Houten et al. [3], evaluating breast tissue are provided. Estimates of the Poisson ratio across specimens provide a useful check.

Discussion and Conclusions

Using noninvasive MRE, we report on the advance of directly estimating two independent material parameters, which is necessary and sufficient to specify the constitutive properties of a solid. This advance was afforded by the ability to simultaneously image ortho-normal acoustic longitudinal and shear waves. The method has proven feasible in an idealized, cylindrical phantom. Further study is needed to determine whether the method can be extended to irregular shaped organs, in vivo, such as the breast or prostate.

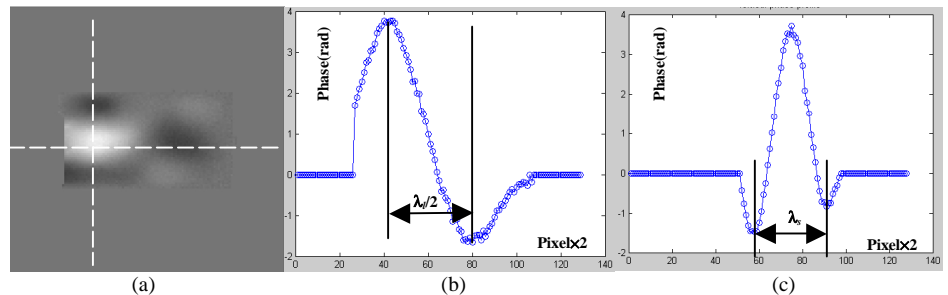
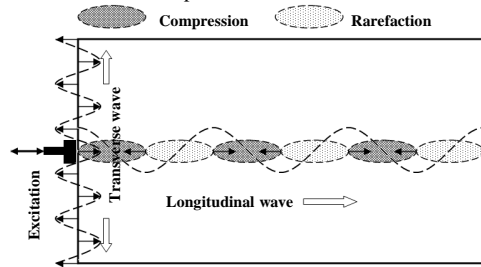


Figure 1: Schematic diagram of wave generation.

Figure 2: Phase map (a), and its horizontal (b) & vertical (c) line profiles for 6% gelatin phantom.

Table 1: Parameters for 6% gelatin vs. breast tissue

Parameter	λ (KPa)	μ (KPa)	Y (KPa)	ν
6% gelatin	14.1 ± 9.1	4.1 ± 1.0	11.8 ± 3.1	0.38 ± 0.09
Fat [3]	39.4 ± 24.5	8.5 ± 1.4	23.5 ± 4.0	0.39 ± 0.06
FBG * [3]	53.6 ± 36.3	9.5 ± 1.5	26.6 ± 4.5	0.40 ± 0.05

* FBG: Fibroglandular tissue

References:

1. Muthupillai R., et al., Science 269: 1854-7, 1995.
2. Oliphant T.E., et al. MRM 45:299-310, 2001.
3. Houten E.E.W.V., et al. JMRI 17:72-85, 2003.
4. Zhang B., et al., Proc. ISMRM 2003.